Antitumor Agents 4. Characterization of Free Radicals Produced during Reduction of the Antitumor Drug 5*H*-Pyridophenoxazin-5-one: An EPR Study

Angelo Alberti,*,‡ Adele Bolognese,*,§ Maurizio Guerra,‡ Antonio Lavecchia,|| Dante Macciantelli,‡ Massimo Marcaccio,⊥ Ettore Novellino,|| and Francesco Paolucci⊥

Istituto per la Sintesi Organica e la Fotoreattività, ISOF-CNR, Via P. Gobetti 101, I-40129 Bologna, Italy, Dipartimento di Chimica Organica e Biochimica, Università di Napoli "Federico II", Via Cynthia 6, Monte Sant'Angelo, I-80126 Napoli, Italy, Dipartimento di Chimica Farmaceutica e Tossicologia, Università di Napoli "Federico II", Via D. Montesano 49, I-80131 Napoli, Italy, and Dipartimento di Chimica "G. Ciamician", Università di Bologna, via Selmi, 2, I-40126 Bologna, Italy

Received April 16, 2003; Revised Manuscript Received August 18, 2003

ABSTRACT: 5*H*-Pyridophenoxazin-5-one (PPH), a new anticancer iminoquinone, is able to inhibit a large number of lymphoblastoid and solid tumor-derived cells at submicromolar concentrations. Molecular modeling calculations indicated that this compound might intercalate into the DNA double strand. This was also supported by nuclear magnetic resonance studies. Since free radicals arising from anticancer quinonic drugs have been proposed to be key species responsible for DNA cleavage, we have aimed to intercept and identify free radicals from PPH generated under bioreductive conditions. The first and second monoelectronic reduction potentials of PPH were measured by means of cyclic voltammetry: the reduction potential of PPH is compatible with its reduction by compounds such as NADH, and suggested that reduction of PPH may play a role in its cytotoxicity. The radical anion $PPH^{\bullet-}$ was detected by means of electron paramagnetic resonance spectroscopy, and its identification was supported by DFT calculations. EPR experiments in the presence of spin traps 5,5-dimethylpyrroline *N*-oxide and 5-(diethoxyphosphoryl)-5-methylpyrroline *N*-oxide suggested the occurrence of an electron transfer between the radical anion of the drug and oxygen resulting in the formation of the superoxide anion ($O_2^{\bullet-}$). The enthalpy of the reaction of $PPH^{\bullet-}$ with O_2 was determined both in the gas phase and in solution at the B3LYP/6-31+G* level using the isodensity PCM method, and the overall process in dimethyl sulfoxide was predicted to be slightly exothermic. We propose that the monoelectronic reduction of PPH in the proximity of DNA may eventually lead to radicals that could cause considerable damage to DNA, thus accounting for the high cytotoxic activity of the drug. Indeed, a comet assay (alkaline single-cell electrophoresis) showed that PPH causes free radical-induced DNA damage.

Anticancer antibiotics are currently the focus of intensive research because of their biological activity and their intricate modes of action. Several antibiotic quinones are known to have significant antitumor properties, mitoxantrone (*1*), doxorubicin (*1*), mitomycin (*2*), streptonigrin (*3*), and actinomycin D (*4*) being typical members of this family. Unfortunately, along with their strong antitumor activity, some members of this group suffer from a delayed toxicity that precludes their use as anticancer agents. A major goal of research in this area is therefore the individuation of compounds that while retaining the biological activity exhibit an enhanced selectivity toward cancer cells.

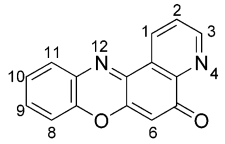

PPH

The antineoplastic activity of these drugs is the result of a strong interaction with DNA in the target cells which causes a degradation of the structure of the nucleic acid and, consequently, terminates its biological function (*5*). The planar system of these drugs can intercalate between the DNA base pairs, where the major contributions to the binding arise from hydrogen bonding and/or electrostatic, van der Waals, and hydrophobic interactions. At the same time, the quinone moiety of these agents can also undergo enzymatic reduction. In the presence of molecular oxygen, the resulting semiquinone and hydroquinone produce reactive oxygen species or ROS[1] (superoxide radical anions, hydrogen peroxide, and hydroxyl radicals) in a process known as redox cycling. ROS are detrimental to cellular macromolecules in that they are capable of causing DNA strand scission, protein

* To whom correspondence should be addressed. A.A.: phone, (39) 051 6398325; fax, (39) 051 6398349; e-mail, aalberti@isof.cnr.it. A.B.: phone, (39) 081 674121; fax, (39) 081 674393; e-mail, bologne@unina.it.

‡ ISOF-CNR.

§ Dipartimento di Chimica Organica e Biochimica, Università di Napoli "Federico II".

|| Dipartimento di Chimica Farmaceutica e Tossicologia, Università di Napoli "Federico II".

⊥ Università di Bologna.

10.1021/bi0346087 CCC: $25.00
Published on Web 09/25/2003

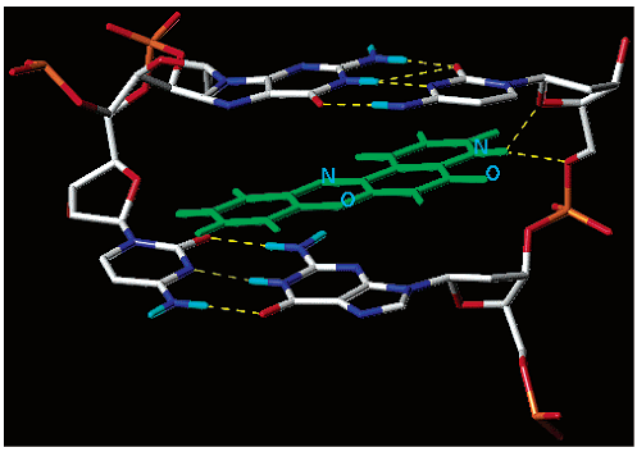

FIGURE 1: Proposed model of PPH intercalated into the [d(GAAGCTTC)]$_2$ octamer. Dashed lines represent hydrogen bonds (taken from ref *6*).

oxidation, and other lesions. The production of semiquinones and/or hydroquinones by enzymatic reduction is strongly dependent on the presence of electron-withdrawing or electron-donating groups on the quinone system.

In recent papers (*6*, *7*), we have described the synthesis and biological activity of PPH, a new anticancer iminoquinone, and of a series of its derivatives that are able to inhibit a large number of lymphoblastoid and solid tumor-derived cells at submicromolar concentrations. Molecular modeling studies and NMR investigations suggested that the cytotoxic activity of PPH results from the intercalation at the middle 5′-G·C-3′ base pairs of DNA (*6*), involving the formation of two strong hydrogen bonds between the hydrogen of the positively charged pyridine nitrogen of protonated PPH and both the O4′ atom in the deoxyribose ring of the cytosine C5 residue and the O5′ atom of the phosphate backbone located between the G4 and C5 residues of a [d(GAAGCTTC)]$_2$ octamer. Additional stability of the complex arises from $\pi-\pi$ stacking interactions between the tetracyclic pyridophenoxazinone system and the aromatic base rings (see Figure 1).

The observation of a DNA intercalating mechanism for PPH does not, however, imply that this is the only mode of action of this iminoquinone. Actually, because the iminoquinone might also participate in single-electron transfer processes, chances are that DNA-cleaving radicals can be generated under bioreductive conditions. Consistently, it has been shown that actinomycin D, a drug containing the phenoxazone system present in PPH, is capable of enzymatic single-electron reduction to a free radical intermediate with subsequent transfer of the electron to oxygen to yield superoxide, according to quinone-containing antibiotics (anthracyclines, mitomycin C, streptonigrin, etc.) (*8*). Besides, coordination of transition metal atoms by the carbonyl group of PPH and the nitrogen of the adjacent pyridine ring may facilitate the occurrence of these SET processes.

In light of the above, we thought it would be advisable to investigate the behavior of PPH toward reducing agents, and we report here on an electrochemical and EPR study of the reduction of PPH with either chemical or biochemical reducing agents in the absence and presence of spin trapping agents. In addition, the DNA-damaging potential of PPH in normal human peripheral blood lymphocytes was investigated by means of alkaline single-cell gel electrophoresis (comet assay) (*9*, *10*).

EXPERIMENTAL PROCEDURES

Materials. PPH was synthesized as previously described (*6*, *7*), while all other chemicals (TBAH, NADH, DMPO, and DEPMPO) were purchased and used as received with the exception of the solvents that were dried through standard procedures. Dry vacuum-distilled DMF was purified using sodium anthracenide to remove any trace of water, proton donors, and oxygen (*11*, *12*). RPMI 1640 medium without L-glutamine, low-melting point and normal-melting point (NMP) agarose, phosphate-buffered saline (PBS), and ethidium bromide were purchased from Sigma (St. Louis, MO).

EPR Experiments. EPR spectra were recorded at room temperature with an upgraded Bruker ER200D-ESP300 spectrometer equipped with a dedicated Bruker ESP 3220 data system for storage and manipulation of the spectra, an NMR gaussmeter for magnetic field calibration, and a frequency counter for the determination of *g* factors that were corrected with respect to that of perylene radical cation in concentrated sulfuric acid. Computer simulations of the spectra were obtained using a software based on a Monte Carlo minimization procedure (*13*). The chemical reduction was carried out in small capillary tubes (inside diameter of 1 mm) by dissolving very small amounts of PPH and ^{t}BuOK or NADH in dry DMSO. The electrochemical experiments were carried out using an Amel Instruments 2051 potentiostat and a flat cell inserted inside the cavity of the EPR spectrometer and equipped with a platinum gauze (cathode) and a platinum wire (anode). For these experiments, PPH ($\sim 10^{-2}$ M) was dissolved in dry DMSO containing Bu_4NClO_4 (10^{-1} M) as the supporting electrolyte. Once the radical anion was observed, a small amount of DMPO or DEPMPO was added to the solution.

DFT Calculations. DFT calculations employing the B3LYP functional (*14*, *15*) were carried out on PPH$^{\bullet-}$ to compute the hfs constants using the GAUSSIAN98 system of programs (*16*). Calculations were performed also on its neutral parent PPH, triplet oxygen ($^3O_2$), and the superoxide radical anion ($O_2^{\bullet-}$) to determine the thermochemistry of the reaction of PPH$^{\bullet-}$ with $^3O_2$. Unrestricted wave functions were used for radical and triplet species. First, geometries of PPH and PPH$^{\bullet-}$ were obtained employing a valence double-ζ basis set supplemented with polarization d-functions on heavy atoms (*17*) (6-31G*). At this level of theory, the radical anion was computed to be thermodynamically stable with respect to its neutral parent so that standard diffuse functions (*18*) were added to heavy atoms to better describe the radical anion in geometry optimization (*19*) (UB3LYP/6-31+G*).

[1] Abbreviations: AEA, adiabatic electron affinity; ^{t}BuOK, potassium *tert*-butoxide; DFT, density functional theory; DMF, dimethylformamide; DMPO, 5,5-dimethyl-1-pyrroline *N*-oxide; DEPMPO, 5-(diethoxyphosphoryl)-5-methyl-1-pyrroline *N*-oxide; DMSO, dimethyl sulfoxide; EPR, electron paramagnetic resonance; hfs, hyperfine splitting; IPCM, isodensity polarizable continuum model; KB, human nasopharyngeal epidermal carcinoma; NMR, nuclear magnetic resonance; NHE, normal hydrogen electrode; PPH, 5*H*-pyridophenoxazin-5-one; ROS, reactive oxygen species; SEM, standard error of the mean; SET, single-electron transfer; TBAH, tetrabutylammonium hexafluorophosphate; TZVP, triple-ζ valence polarized; VEA, vertical electron affinity; ZPVE, zero-point vibrational energy.

The vertical (VEA) and adiabatic (AEA) electron affinities remain largely negative also at this level of theory, being −1.79 and −1.97 eV, respectively. Hfs constants for $PPH^{\bullet-}$ were computed at the B3LYP/6-31+G* geometry level using a DFT-optimized valence triple-ζ basis set (TZVP) (*20*) with addition of a tight s-function to the core orbitals of heavy atoms that was shown to provide good hfs constants in other instances (*21*, *22*). The basis set was augmented with standard diffuse functions to better describe the radical anion. The effect of solvent was taken into account by the polarizable continuum model (PCM) (*23*) by employing the dielectric constant ϵ of DMSO ($\epsilon = 46.7$). The enthalpy of the reaction of $PPH^{\bullet-}$ with $^3O_2$ was determined both in the gas phase and in solution at the B3LYP/6-31+G* level using the isodensity PCM method (IPCM).

Electrochemistry. The electrochemical experiments (DMF/TBAH) were carried out in an airtight single-compartment cell described elsewhere (*11*, *24*). The working electrode was either a microelectrode (0.5 mm diameter platinum wire sealed in glass) or an ultra-microelectrode (either 125 or 25 μm diameter platinum disk); the counter electrode consisted of a platinum spiral, and the quasi-reference electrode was a silver spiral. The drift of the quasi-reference electrode was negligible for the time required for an experiment.

The cell containing the supporting electrolyte and the electroactive compound was dried under vacuum at 110−120 °C for at least 60 h before each experiment. The pressure measured in the electrochemical cell prior to performance of the trap-to-trap distillation of the solvent was typically $1-2 \times 10^{-5}$ mbar.

All the $E_{1/2}$ potentials are referred to a normal hydrogen electrode, and the corresponding values were determined by adding ferrocene (whose $E_{1/2} = 0.674$ V vs NHE) as an internal standard (*25*). Voltammograms were recorded with an AMEL model 552 potentiostat or a custom-made fast potentiostat controlled by either an AMEL model 568 function generator or an ELCHEMA model FG-206F instrument. The positive-feedback circuit of the potentiostat achieved the minimization of the uncompensated resistance effect in the voltammetric measurements. The data acquisition was performed with a Nicolet model 3091 digital oscilloscope interfaced with a personal computer. Temperature control within 0.1 °C was accomplished with a Lauda Klein-Kryomat thermostat.

Cells. Blood was obtained from young, male, healthy, nonsmoking donors. Peripheral blood lymphocytes were isolated by centrifugation in a density gradient of Gradisol L (15 min at 280*g*). The viability of the cells was measured by the trypan blue exclusion method and was found to be ∼99%. Lymphocytes accounted for ∼92% of the leukocytes in the obtained cell suspension as judged by the characteristic shape of the nucleus. The final concentration of the lymphocytes was adjusted to $1-3 \times 10^5$ cells/mL by adding RPMI 1640 to the single-cell suspension.

Cell Treatment. PPH was taken from a stock (0.5 mM) RPMI 1640 solution and added to the suspension of the cells to give a final concentration in the range of 0.01−5 μM. The control cells received only RPMI medium. The RPMI, as stated by the manufacturer (Sigma), was without antibiotics and serum supplement. To examine DNA damage, the lymphocytes were incubated with the drug for 1 h at 37 °C. Each experiment included a positive control, which was H_2O_2 at 10 μM. H_2O_2 produced pronounced DNA damage, which resulted in ∼30% tail DNA.

Cell Viability. Cell viability was determined by trypan blue exclusion analysis. Lymphocytes were incubated with PPH at concentrations in the range of 0.01−100 μM for 1 h at 37 °C, washed, and resuspended in RPMI 1640. An equal volume of 0.4% trypan blue reagent was added to a cell suspension, and the percentage of viable cells was evaluated under a field microscope. Assays were performed in triplicate. The viability of the lymphocytes was checked concurrently in all experiments in the appropriate concentration range.

Comet Assay. The comet assay was performed under alkaline conditions according to the procedure of Singh et al. (*9*) with modifications (*26*−*28*). A freshly prepared suspension of cells in 0.75% low-melting point agarose dissolved in PBS was spread onto microscope slides precoated with 0.5% normal-melting point agarose. The cells were then lysed for 1 h at 4 °C in a buffer consisting of 2.5 M NaCl, 100 mM EDTA, 1% Triton X-100, and 10 mM Tris (pH 10). After the lysis, the slides were placed in an electrophoresis unit, and the DNA was allowed to unwind for 40 min in the electrophoretic solution consisting of 300 mM NaOH and 1 mM EDTA (pH >13). Electrophoresis was carried out at 4 °C for 25 min and at 30 V (1 V/cm) by using an Amersham Pharmacia Biotech power supply and adjusting the current to 300 mA by increasing or reducing the buffer level. The slides were then neutralized with 0.4 M Tris (pH 7.5), stained with 12 μg/mL ethidium bromide, and covered with cover slips. To prevent additional DNA damage, all the steps described above were conducted under dimmed light or in darkness.

Comet Analysis. The objects were observed at 200× magnification with an Olympus fluorescent microscope equipped with a 100 W mercury lamp. Images were captured by a monochrome CCD camera (Cohu Electronic Division, San Diego, CA). Imaging was performed using a computerized image analysis system from Delta Sistemi (Rome, Italy) which acquires images, computes the integrated intensity profile for each cell, estimates the comet cell head and tail components, and then evaluates a range of derived parameters. Fifty images were randomly selected from each sample, and the percentage of DNA in the tail (% tail DNA) was measured. Two parallel tests with aliquots of the same sample of cells were performed for a total of 100 cells. Three comet parameters were analyzed: a measure of tail length (measured from the center of the comet head), % tail DNA, and tail moment (a measure of tail length × % tail DNA). The % tail DNA is positively correlated with the level of DNA breakage or/and alkali labile sites in the cell and is negatively correlated with the level of DNA cross-links (*29*). The mean value of the % tail DNA in a particular sample was taken to be an index of DNA damage in this sample and was used to display the results of all experiments, but the results of DNA damage caused by PPH alone were presented also numerically in terms of all three parameters to facilitate external evaluation of the data. Because our measurement system was not calibrated, tail length and tail moment were presented in arbitrary units. The values in this study were expressed as the mean ± SEM from two separate experiments; i.e., data from two experiments were pooled and the statistical parameters calculated. In the cell viability study, all experi-

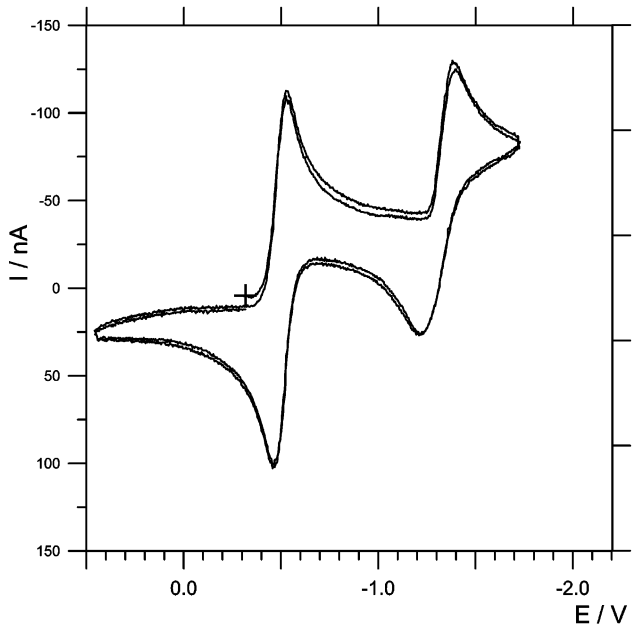

FIGURE 2: Cyclic voltammetric curve for 1 mM PPH in a 0.07 M TBAH/DMF solution, with a scan rate of 1 V/s and a *T* of 24 °C (working electrode, Pt disk 125 μm in diameter).

ments were performed in triplicate. The data were analyzed using Statistica (StatSoft, Tulsa, OK). If no significant differences between variations were found, as assessed by the Snedecor−Fisher test, the differences between means were evaluated by applying the two-tailed Student's *t* test. Otherwise, the Cochran−Cox test was used.

RESULTS AND DISCUSSION

The electrochemical behavior of PPH was investigated by means of cyclic voltammetry in a DMF solution at low and room temperature under highly aprotic conditions. The voltammetric curve recorded at room temperature with a platinum ultra-microelectrode at a scan rate of 1 V/s showed a first reduction wave with an $E_{1/2}$ of −0.496 V (vs NHE). This corresponded to a fully reversible monoelectronic process leading to the formation of the radical anion $PPH^{\bullet -}$. A second monoelectronic reduction wave was also observed at more negative potentials ($E_{1/2}$ = −1.306 V vs NHE), reflecting the occurrence of what appeared to be a rather sluggish electron transfer (see Figure 2). When PPH was electrochemically reduced in a DMSO solution inside the cavity of an EPR spectrometer, a rather intense and complex spectrum was observed (Figure 3a) that could be satisfactorily interpreted (Figure 3b) on the basis of the spectral parameters collected in Table 1 and indicating coupling of the unpaired electron with eight hydrogen and two nitrogen atoms. On this basis, the spectrum is attributed to the radical anion of PPH. The attribution is supported by the similarity of these values with those predicted for the radical anion by means of DFT calculations and also collected in Table 1. The finding that a fairly similar spectrum was observed when PPH was reacted with potassium *tert*-butoxide in DMSO further substantiates the identification of the radical anion. The only significant difference between the spectra observed upon chemical and electrochemical reduction was to be found in the splitting of N_{10}, whose larger value in the former case

Table 1: Experimental and Calculated Hfs Constants for the Radical Anion of PPH[a,b]

	DFT calculations[c]	electrochemical reduction/DMSO	^{t}BuOK/ DMSO	NADH/ DMSO
$a(H_1)$	−0.32	0.29	0.22	nr[d]
$a(H_2)$	−0.23	0.26	nr[d]	nr[d]
$a(H_3)$	−0.91	0.78	0.53	0.79
$a(H_6)$[e]	−0.49	0.36	0.33	0.65
$a(H_8)$[e]	0.65	0.33	0.28	0.63
$a(H_9)$	−2.59	2.34	2.31	2.50
$a(H_{10})$	0.90	0.64	0.41	0.71
$a(H_{11})$	−3.11	3.07	2.80	3.02
$a(N_4)$	−0.40	0.49	0.35	0.65
$a(N_{12})$	6.01	6.30	6.97	7.05

[a] Values in gauss = 10^{-4} T. [b] g = 2.0038(4). [c] Computed at the PCM(ϵ=DMSO)/UB3LYP/VTZP+1s+diffuse//UB3LYP/6-31+G* level. [d] Not resolved. [e] The assignment of these two hfs constants was reversed since the B3LYP functional was found to overestimate the small positive hydrogen hfs constants in delocalized π systems by a factor of ca. 1.5 (*31*).

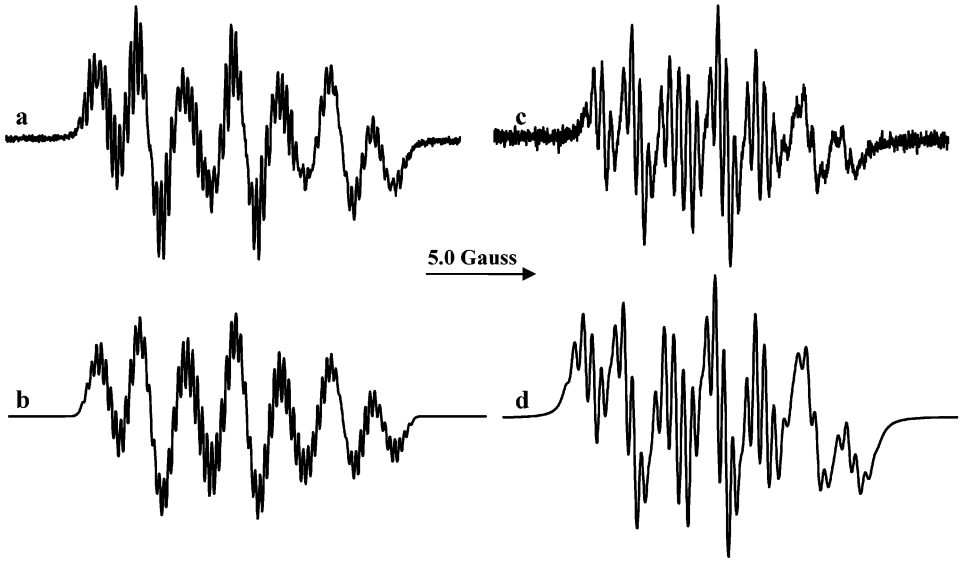

FIGURE 3: Experimental and computer-simulated EPR spectra observed by electrochemical reduction of PPH in deoxygenated DMSO containing some Bu_4NClO_4 (a and b) and by reaction of PPH with NADH in DMSO (c and d) at room temperature. Spectra a and c are experimental spectra and spectra b and d the corresponding simulations. The spectral intensity is in arbitrary units.

is to be attributed to the greater polarity of the medium caused by the presence of the butoxide anions.

As PPH includes in its molecule a quinoniminic system, it is not surprising that it is readily reduced to the corresponding radical anion under mild reducing conditions. Spectra similar to those shown in Figure 3a, although characterized by a much worse resolution, could also be observed by treating PPH with sodium borohydride in aqueous ethanol or by reaction with NADH in DMSO (Figure 3c). EPR spectra could also be observed by treating PPH with a copper(I) salt, namely, CuCl, in either DMSO or ethanol. In this case, the spectra exhibited the typical spectral pattern of a Cu(II) complex (*30*) and consisted of four equally spaced lines with decreasing line width with increasing field [$a(^{29}Cu) = 5.717$ mT] and with a g factor value of 2.1613(6).

As already mentioned, the biological activity of PPH is believed to be mostly due to its intercalation within DNA, but it is also possible that its ability to originate ROS, and ultimately •OH radicals, also contributes to some extent to its antitumor activity. If this were the case, the process leading to ROS would probably involve as a first step the formation of the $PPH^{\bullet-}$ radical anion at the expense of some reducing agent present in the biological system or of the protein-bound transition metal atoms. These possibilities are substantiated by our observation of the copper(II) EPR spectrum when PPH reacts with a copper(I) salt and of the $PPH^{\bullet-}$ spectrum when it reacts with NADH. The superoxide anion would subsequently form *via* a single electron transfer (SET) from $PPH^{\bullet-}$ to the oxygen present in the environment.

The reaction between $PPH^{\bullet-}$ and O_2 can be indirectly followed experimentally using EPR spectroscopy by intercepting some of the intervening radical species, and in particular the superoxide radical anion. Because $O_2^{\bullet-}$ cannot be detected directly, in conjunction with EPR spectroscopy the spin trapping technique must be used, whereby a transient undetectable paramagnetic species is scavenged by an appropriate molecule (called the spin trap) introduced into the system and is converted to a longer-lived and EPR detectable radical adduct (*32*, *33*). Among the many spin traps that have been developed since this technique was first introduced in the early 1970s, DMPO is especially suitable for biological studies because it is soluble in aqueous media and readily traps oxygen-centered radicals, such as $O_2^{\bullet-}$, •OR, and •OH, affording easily identifiable adducts (*34*; ref *35* and references therein).

Aerobic electrolysis of a DMSO solution of PPH inside the cavity of the EPR spectrometer led to the observation of the poorly resolved spectrum of $PPH^{\bullet-}$ shown in Figure 4a. Addition of a small amount of DMPO to the solution resulted in the appearance of new lines on the wings of the spectrum of the radical anion (Figure 4b). The hyperfine spectral parameters indicate that these new lines are due to the spectrum of the DMPO adduct of the superoxide radical anion, which, because of the residual humidity of DMSO, is present in its protonated form. As time goes by and following a further addition of DMPO, the clean spectrum of the DMPO−OOH adduct is observed (Figure 4c). After some additional time, some extra lines appear indicating the presence of the unprotonated $DMPO-O_2^-$ adduct (Figure 4d). After a longer time interval, the spectral pattern is again dominated by the signal from the PPH radical anion (Figure 4e), while a small amount of the $DMPO-O_2^-$ adduct remains detectable.

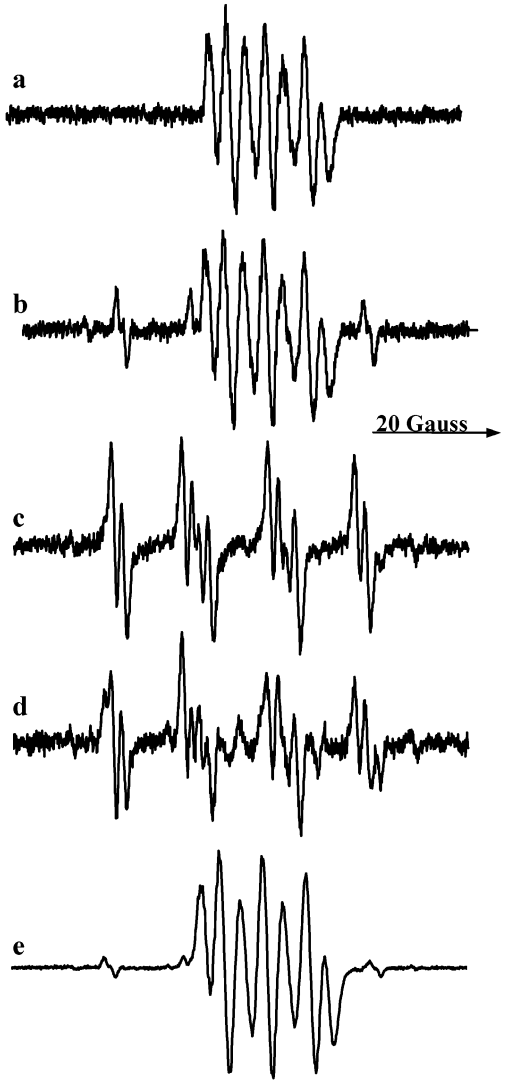

FIGURE 4: EPR spectra observed upon aerobic electrochemical reduction of PPH in DMSO before and after addition of a small amount of the spin trap DMPO: (a) in the absence of DMPO and (b) DMPO added, (c) same as spectrum b after 5 min, (d) same as spectrum b after 25 min, and (e) same as spectrum b after 31 min. The spectral intensity is in arbitrary units.

An admission that, after the reduction of PPH in the aerobic system, the resulting radical anion reacts with oxygen to form the superoxide radical anion can account for the spectral sequence shown in Figure 4. This species, which is elusive under the normal electrolytic conditions, is readily trapped by DMPO to give the corresponding $DMPO-O_2^-$ adduct that is quickly protonated to the $DMPO-O_2H$ adduct [$a(N) = 12.74$ G, $a(H_2) = 10.38$ G, $a(H_3) = 1.45$ G, and $g = 2.0060(3)$] by the water present in traces in the anhydrous DMSO. As all the water is consumed, the additional superoxide anion is trapped in the unprotonated form and the spectrum of the $DMPO-O_2^-$ adduct becomes detectable [$a(N) = 13.74$ G, $a(H_2) = 11.74$ G, $a(H_3) = 0.84$ G, and $g = 2.0059(4)$]. When all the oxygen has been eventually consumed, the PPH^- radical anion does not undergo any further reaction and its spectrum is again observed while those of the $DMPO-O_2H$ and $DMPO-O_2^-$ adducts become vanishingly small.

Scheme 1

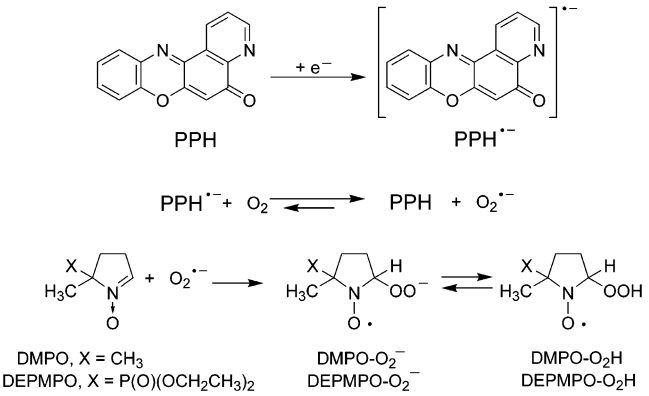

The correct identification of the signals due to the DMPO−O_2^- and DMPO−O_2H adducts was achieved by adding a small amount of water to the solution being electrolytically reduced. Actually, the addition of water led to the observation of a clean spectrum of the hydroperoxyl adduct identical to that shown in Figure 4c. Consistently, replacing DMPO with DEPMPO, another spin trap particularly suitable for the detection of the superoxide radical (*36*−*38*), resulted in the detection of both the DEMPO−OOH adduct [a(N) = 12.38 G, a(H_2) = 11.06 G, a(^{31}P) = 49.10 G, and g = 2.0064(3)] and the DEPMPO−O_2^- adduct [a(N) = 13.19 G, a(H_2) = 10.86 G, a(^{31}P) = 48.81 G, and g = 2.0064(0)] adducts (see Scheme 1).

While it is known that the superoxide anion in a biological environment naturally evolves to the hydroxyl radical •OH, in our study the formation of a DMPO−OH adduct could not be evidenced. On the other hand, this is most likely due to the fact that our electrochemical reduction is carried out in DMSO, a medium that readily quenches hydroxyl radicals.

The chemistry outlined in Scheme 1 requires that all of the intervening species have appropriate reduction or oxidation potentials; in particular, the oxidation potential of PPH$^{\bullet-}$ and the reduction potential of O_2 must be compatible. We have measured the former potential as −0.496 V in DMF vs NHE (see above), whereas the latter has been reported to be −0.726 V (also in DMF vs NHE). Given these values, the easiness of the SET process may be estimated using the Marcus theory that in its simplified form is given as eq 1 (*39*, *40*).

$$\Delta G^{\ddagger} = \lambda/4(1 + \Delta G^{\circ}/\lambda)^2 \qquad (1)$$

Using values of 33.8 kcal/mol (*41*) for the overall reorganization energy (λ) of the system and 5.30 kcal/mol for a ΔG° of 23.06(E_{ox} − E_{red}), a value of 11.31 kcal/mol is obtained for $\Delta G^{\ddagger}$ which would suggest that formation of the superoxide anion is a rather slow process. It should, however, be noted that the second step of Scheme 1 is not a proper equilibrium, because the $O_2^{\bullet-}$ when formed is immediately extracted from the system, due to conversion to •O_2H in the biological media or to trapping by DMPO (or DEPMPO) in our EPR experiments.

The overall thermodynamic feasibility of the electron transfer process was more accurately estimated through a computational approach that considered the process both in the gas phase and in the presence of a solvent (DMSO). The enthalpy H_r for the SET reaction was computed with the DFT method. At the B3LYP/6-31+G* level, the electron transfer process is considerably endothermic (H_r = 1.38 eV). Inclusion of the estimated vibrational energy contribution (ZPVE) has little effect (H_r = 1.43 eV). It is, however, expected that solvation should favor electron transfer, and indeed, the SET process is predicted to become slightly exothermic if the effect of the solvent (DMSO) is taken into account using the isodensity polarizable continuum model (IPCM). In this case, H_r was computed to be −0.08 eV at the IPCM(ϵ=DMSO)/B3LYP/6-31+G*//B3LYP/6-31+G* level.

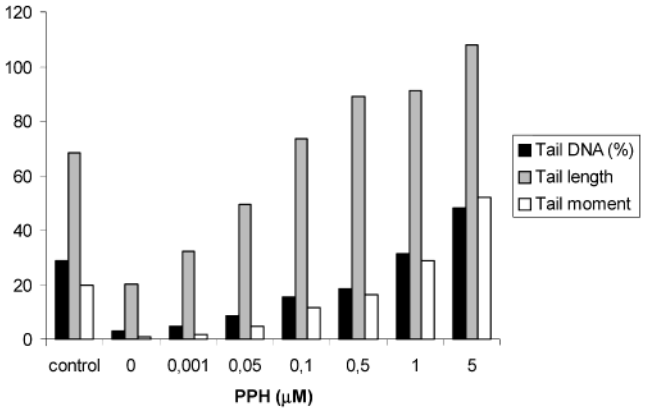

FIGURE 5: Mean comet of tail DNA (percentage), tail length (micrometers), and tail moment (micrometers) of human lymphocytes exposed for 1 h at 37 °C to PPH. The number of cells in each treatment was 100.

In light of the experimental and computational evidence reported above, the cytotoxic activity of PPH might be associated with a ROS-mediated mechanism. Therefore, it seemed of interest to examine the ability of PPH to cause oxidative DNA damage by single-cell gel electrophoresis or a comet assay. In this assay, DNA breakage in individual cells is detected by alkaline lysis in gels on microscope slides, followed by electrophoresis, which draws DNA fragments out of nuclei to form comet-like tails. Comets are stained with ethidium, and the tail moment is determined using an image analysis system. The alkaline comet assay has been also used for several years as a method for quantitation of oxidized bases in DNA (*26*).

The lymphocyte viability tests after incubation with PPH in the concentration range of 0.01−100 μM showed a concentration-dependent decrease in cell viability, more than 50% of the cell population having died at 100 μM PPH. In experiments in the concentration range of 0.01−5 μM, the viability of the lymphocytes was greater than 80%. The measurements of the viability of lymphocyte cells in each subsequent experiment at applied concentrations of the chemical that was used always gave a viability of greater than 80%. The mean % tail DNA, tail length, and tail moment for the lymphocytes exposed for 1 h to PPH are shown in Figure 5, while Table 2 lists the numerical values for tail length, tail moment, and % tail DNA. The significant increase in % tail DNA with the drug dose in the range of 0.01−5 μM is evident. The observed trend might be due to the induction of DNA strand breaks and/or the formation of alkali labile sites, which can be transformed into strand breaks in the alkaline comet assay. The breaks or alkali labile

Table 2: Percentage of DNA in Tail, Tail Length, and Tail Moment of Human Lymphocytes Exposed for 1 h at 37 °C to PPH [mean ± SEM ($n = 100$)]

[PPH] (μM)	tail DNA (%)	tail length (μm)	tail moment (μm)
positive control[a]	28.7 ± 1.9	68.5 ± 1.8	19.8 ± 1.3
0	2.99 ± 0.98	20.2 ± 1.6	0.80 ± 0.31
0.001	4.85 ± 0.43	32.4 ± 3.9	1.77 ± 1.15
0.05	8.75 ± 1.31	49.4 ± 3.3	4.52 ± 0.91
0.1	15.6 ± 1.2	73.5 ± 2.5	11.6 ± 1.3
0.5	18.3 ± 2.1	89.2 ± 4.2	16.5 ± 1.6
1	31.4 ± 2.3	91 ± 3	28.7 ± 3.2
5	48.2 ± 3.2	108 ± 4	52.2 ± 3.9

[a] In 10 μM H_2O_2 for 5 min at 37 °C.

sites may be a result of the action of ROS that are formed during the metabolism of PPH in the cell.

CONCLUSIONS

Some anticancer quinone drugs binding to DNA have been reported to be topoisomerase inhibitors. The high antiproliferative activity of PPH and its derivatives against numerous human solid and liquid tumor cells seems, however, to reflect its ability to intercalate into DNA rather than its selective targeting of topoisomerases, consistent with the finding that PPH has no effect on the catalytic activity of topoisomerase I or II, being unable to significantly increase the amount of protein-linked DNA breaks in KB cells. On the other hand, it is known that the bioreduction of a large number of anticancer agents containing quinone and iminoquinone groups generates semiquinone radicals which, giving rise to production of ROS, damage DNA.

Cyclic voltammetry of PPH indicates that indeed PPH can be reduced at potentials consistent with bioreduction in the cell. EPR results support a ROS-mediated mechanism of DNA cleavage deriving from bioreduction of PPH. The comet assay results showed that lymphocytes exposed to PPH display a greater extent of DNA damage than those not treated with the drug. These findings argue strongly that oxidative stress is an important mechanism of PPH cytotoxicity. On the other hand, ROS, which have been reported to react with the closest neighboring molecules (*42*), are thought to abstract H^+ from the deoxyribose sugars of either purine or pyrimidine bases of DNA, forming random single-strand breaks. Molecular modeling studies and UV and NMR investigations revealed the ability of PPH to intercalate into DNA, increasing the likelihood that ROS formed as a result of drug reduction would directly affect DNA double strands. This behavior of PPH is similar to that of doxorubicin, daunomycin, and actinomycin D, whose reduction has been reported to contribute to DNA cleavage and, ultimately, to their cytotoxicity (*43*).

ACKNOWLEDGMENT

We thank Dr. Maria Rosaria Scarfì at the Istituto di Ricerca per l'Elettromagnetismo e i Componenti Elettronici (IRECE-CNR, Napoli, Italy) for her precious help with the comet assay and statistical analysis.

REFERENCES

1. Lown, J. W. (1988) in *Anthracycline and Anthracenedione-based Anticancer Agents*, Elsevier, Amsterdam.
2. Carter, S. K., and Crooke, S. T. (1979) *Mitomycin C: Current Status and New Developments*, Academic Press, New York.
3. Rao, K. V., and Cullen, W. P. (1960) in *Antibiotics Annual 1959−1960* (Welch, H., and Marti-Ibanez, F., Eds.) Medical Encyclopedia, New York.
4. Wakelin, L. P. G., and Waring, M. J. (1990) in *Comprehensive Medicinal Chemistry* (Sammes, P. G., Ed.) Vol. 2, pp 703−724, Pergamon Press, Oxford, U.K.
5. Chabner, B. A., Allegra, C. J., Curt, G. A., and Calabresi, P. (1996) in *Goodman and Gilman's The Pharmacological Basis of Therapeutics* (Hardman, J. G., Limbird, L. E., Molinoff, P. B., Ruddon, R. W., and Gilman, A. G., Eds.) 9th ed., pp 1233−1287, McGraw-Hill, New York.
6. Bolognese, A., Correale, G., Manfra, M., Lavecchia, A., Mazzoni, O., Novellino, E., Barone, V., La Colla, P., Loddo, R., Murgioni, C., Pani, A., Serra, I., and Setzu, G. (2002) *J. Med. Chem. 45*, 5205−5216.
7. Bolognese, A., Correale, G., Manfra, M., Lavecchia, A., Mazzoni, O., Novellino, E., Barone, V., La Colla, P., and Loddo, R. (2002) *J. Med. Chem. 45*, 5217−5223.
8. Nakazawa, H., Chou, E. F., Andrews, A. P., and Bachur, R. N. (1981) *J. Org. Chem. 46*, 1493−1496.
9. Singh, N. P., McCoy, T., Tice, R. R., and Schneider, E. L. (1988) *Exp. Cell Res. 175*, 184−192.
10. Fairbairn, D. W., Olive, P. L., and O'Neill, K. L. (1995) *Mutat. Res. 339*, 37−59.
11. Marcaccio, M., Paolucci, F., Paradisi, C., Carano, M., Roffia, S., Fontanesi, C., Yellowlees, L. J., Serroni, S., Campagna, S., and Balzani, V. (2002) *J. Electroanal. Chem. 532*, 99−112.
12. Saji, T., Yamada, T., and Aoyagui, S. (1975) *J. Electroanal. Chem. 61*, 147−153.
13. Lucarini, M., Luppi, B., Pedulli, G. F., and Roberts, B. P. (1999) *Chem. Eur. J. 5*, 2048−2054.
14. Becke, A. D. (1993) *J. Chem. Phys. 98*, 5648−5652.
15. Lee, C., Yang, W., and Parr, R. G.(1988) *Phys. Rev. B 37*, 785−794.
16. Frisch, M. J., Trucks, G. W., Schlegel, H. B., Scuseria, G. E., Robb, M. A., Cheeseman, J. R., Zakrzewski, V. G., Montgomery, J. A., Jr., Stratmann, R. E., Burant, J. C., Dapprich, S., Millam, J. M., Daniels, A. D., Kudin, K. N., Strain, M. C., Farkas, O., Tomasi, J., Barone, V., Cossi, M., Cammi, R., Mennucci, B., Pomelli, C., Adamo, C., Clifford, S., Ochterski, J., Petersson, G. A., Ayala, P. Y., Cui, Q., Morokuma, K., Malick, D. K., Rabuck, A. D., Raghavachari, K., Foresman, J. B., Cioslowski, J., Ortiz, J. V., Stefanov, B. B., Liu, G., Liashenko, A., Piskorz, P., Komaromi, I., Gomperts, R., Martin, R. L., Fox, D. J., Keith, T., Al-Laham, M. A., Peng, C. Y., Nanayakkara, A., Gonzalez, C., Challacombe, M., Gill, P. M. W., Johnson, B., Chen, W., Wong, M. W., Andres, J. L., Gonzalez, C., Head-Gordon, M., Replogle, E. S., and Pople, J. A. (1998) *Gaussian 98*, revision A.7, Gaussian, Inc., Pittsburgh, PA.
17. Hariharan, P. C., and Pople, J. A. (1973) *Theor. Chim. Acta 28*, 213−222.
18. Clark, T., Chandrasekhar, J., and Schleyer, P. v. R. (1983) *J. Comput. Chem. 4*, 294−301.
19. Guerra, M. (1999) *J. Phys. Chem. A 103*, 5983−5988.
20. Godbout, N., Salahub, D. R., Andzelm, J., and Wimmer, E. (1992) *Can. J. Chem. 70*, 560−571.
21. Nguyen, M. T., Creve, S., and Vanquickenborne, L. G. (1997) *J. Phys. Chem. A 101*, 3174−3181.
22. Alberti, A., Benaglia, M., Guerra, M., Hudson, A., and Macciantelli, D. (1999) *J. Chem. Soc., Perkin Trans. 2*, 1567−1568.
23. Cossi, M., Barone, V., Cammi, R., and Tomasi, J. (1996) *Chem. Phys. Lett. 255*, 327−335.
24. Paolucci, F., Marcaccio, M., Roffia, S., Orlandi, G., Zerbetto, F., Prato, M., Maggini, M., and Scorrano, G. (1995) *J. Am. Chem. Soc. 117*, 6572−6580.
25. Kuwana, T., Bublitz, D. E., and Hoh, G. J. (1960) *J. Am. Chem. Soc. 82*, 5811−5817.
26. Collins, A. R., Duthie, S. J., and Dobson, V. L. (1993) *Carcinogenesis 14*, 1733−1735.
27. Klaude, M., Eriksson, S., Nygren, J., and Ahnstrom, G. (1996) *Mutat. Res. 363*, 89−96.
28. Błasiak, J., and Kowalik, J. (2000) *Mutat. Res. 469*, 135−145.
29. Ashby, J. A., Tinwell, H., Lefevre, P. A., and Browne, M. A. (1995) *Mutagenesis 10*, 85−90.
30. Fischer, H., and Hellwege, K.-H., Eds. (1977) *Magnetic Properties of Free Radicals*, Landolt-Börnstein, New Series, Group II, Vol.

9, Part a, Springer-Verlag, Heidelberg, Germany. Fischer, H., Ed. (1987) *Magnetic Properties of Free Radicals*, Landolt-Börnstein, New Series, Group II, Vol. 17, Part a, Springer-Verlag, Heidelberg, Germany.
31. Eriksson, L. A. (1997) *Mol. Phys. 91*, 827−833.
32. Janzen, E. G. (1971) *Acc. Chem. Res. 4*, 31−40.
33. Perkins, M. J. (1980) *Adv. Phys. Org. Chem. 17*, 1−64.
34. Mason, R. P. (1984) in *Spin Labeling in Pharmacology* (Holtzman, J. L., Ed.) Vol. 87, Academic Press, New York.
35. Buettner, G. R., and Mason, R. P. (1990) *Methods Enzymol. 186*, 127.
36. Fréjaville, C., Karoui, H., Tuccio, B., Le Moigne, F., Pietri, S., Culcasi, M., Lauricella, R., and Tordo, P. (1994) *J. Chem. Soc., Chem. Commun.*, 1793−1794.
37. Fréjaville, C., Karoui, H., Tuccio, B., Le Moigne, F., Pietri, S., Culcasi, M., Lauricella, R., and Tordo, P. (1995) *J. Med. Chem. 38*, 258−265.
38. Clément, J.-L., Gilbert, B. C., Rockenbauer, A., and Tordo, P. (2001) *J. Chem. Soc., Perkin Trans. 2*, 1463−1470.
39. Eberson, L. (1987) in *Electron-Transfer Reactions in Organic Chemistry*, Springer-Verlag, Heidelberg, Germany.
40. Eberson, L., and Greci, L. (1984) *J. Org. Chem. 49*, 2135−2139.
41. Petrucci, R., Giorgini, E., Damiani, E., Carloni, P., Marrosu, G., Trazza, A., Littaru, G. P., and Greci, L. (2000) *Res. Chem. Intermed. 26*, 269−282.
42. Schraufstatter, I., Hyslop, P. A., Jackson, J. H., and Cochrane, C. G. (1988) *J. Clin. Invest. 82*, 1040−1050. Bolognese, A. Unpublished results.
43. Kohen, R. (1993) *J. Pharmacol. Toxicol. Methods 29*, 185−193.

BI0346087